Westinghouse Non-Proprietary Class 3

WCAP-15435
Revision 1

Technical Justification for Eliminating Pressurizer Surge Line Rupture as the Structural Design Basis for D. C. Cook Units 1 and 2 Nuclear Power Plants

Westinghouse Electric Company LLC

WCAP-15435 Revision 1

Technical Justification for Eliminating Pressurizer Surge Line Rupture as the Structural Design Basis for D. C. Cook Units 1 and 2 Nuclear Power Plants

D. C. Bhowmick
C. K. Ng

August 2000

Verified: _____
J.F. Petsche
Structural Mechanics Technology

Approved: _____
S. A. Swamy, Manager
Structural Mechanics Technology

Westinghouse Electric Company LLC
P.O. Box 355
Pittsburgh, PA 15230-0355

TABLE OF CONTENTS

LIST OF TABLES v

LIST OF FIGURES vi

1 INTRODUCTION 1-1
- 1.1 BACKGROUND 1-1
- 1.2 SCOPE AND OBJECTIVE 1-1
- 1.3 REFERENCES 1-2

2 OPERATION AND STABILITY OF THE PRESSURIZER SURGE LINE AND THE REACTOR COOLANT SYSTEM 2-1
- 2.1 STRESS CORROSION CRACKING 2-1
- 2.2 WATER HAMMER 2-2
- 2.3 LOW CYCLE AND HIGH CYCLE FATIGUE 2-3
- 2.4 SUMMARY EVALUATION OF SURGE LINE FOR POTENTIAL DEGRADATION DURING SERVICE 2-3
- 2.5 REFERENCES 2-4

3 MATERIAL CHARACTERIZATION 3-1
- 3.1 PIPE MATERIAL AND WELDING PROCESS 3-1
- 3.2 MATERIAL PROPERTIES 3-1
- 3.3 REFERENCES 3-1

4 LOADS FOR FRACTURE MECHANICS ANALYSIS 4-1
- 4.1 NATURE OF THE LOADS 4-1
- 4.2 LOADS FOR CRACK STABILITY ANALYSIS 4-2
- 4.3 LOADS FOR LEAK RATE EVALUATION 4-2
- 4.4 LOADING CONDITIONS 4-2
- 4.5 SUMMARY OF LOADS 4-4
- 4.6 GOVERNING LOCATION 4-4
- 4.7 REFERENCES 4-4

5 FRACTURE MECHANICS EVALUATION 5-1
- 5.1 GLOBAL FAILURE MECHANISM 5-1
- 5.2 LEAK RATE PREDICTIONS 5-2
  - 5.2.1 General Considerations 5-2
  - 5.2.2 Calculation Method 5-2
  - 5.2.3 Leak Rate Calculations 5-3

TABLE OF CONTENTS(CONT'D)

5.3 STABILITY EVALUATION 5-4
5.4 REFERENCES 5-4

6 ASSESSMENT OF FATIGUE CRACK GROWTH 6-1

6.1 INTRODUCTION 6-1

7 ASSESSMENT OF MARGINS 7-1

8 CONCLUSIONS 8-1

APPENDIX A - LIMIT MOMENT A-1

LIST OF TABLES

Table 3-1 Room Temperature Mechanical Properties of the Pressurizer Surge Line Materials 3-2

Table 3-2 Representative Tensile Properties 3-3

Table 3-3 Modulus of Elasticity (E) 3-3

Table 4-1 Types of Loadings 4-5

Table 4-2 Normal and Faulted Loading Cases for Leak-Before-Break Evaluations 4-6

Table 4-3 Associated Load Cases for Analyses 4-7

Table 4-4 Summary of Leak-Before-Break Loads and Stresses by Case for Governing Location 4-8

Table 5-1 Leakage Flaw Size 5-6

Table 5-2 Summary of Critical Flaw Size 5-6

Table 6-1 Fatigue Crack Growth Results for 10% of Wall Initial Flaw Size 6-2

Table 7-1 Leakage Flaw Sizes, Critical Flaw Sizes and Margins 7-2

Table 7-2 Leak-Before-Break Conservatisms 7-2

LIST OF FIGURES

Figure 3-1 D. C. Cook Units 1 and 2 Surge Lines Layout 3-4

Figure 4-1 D. C. Cook Units 1 and 2 Surge Lines Showing Governing Location 4-9

Figure 5-1 Fully Plastic Stress Distribution 5-7

Figure 5-2 Analytical Predictions of Critical Flow Rates of Steam-Water Mixtures 5-8

Figure 5-3 [ ]a,c,e Pressure Ratio as a Function of L/D 5-9

Figure 5-4 Idealized Pressure Drop Profile Through a Postulated Crack 5-10

Figure 5-5 Loads Acting on the Model at the Governing Location 5-11

Figure 5-6 Critical Flaw Size Prediction for Node 1020 Case D 5-12

Figure 5-7 Critical Flaw Size Prediction for Node 1020 Case E 5-13

Figure 5-8 Critical Flaw Size Prediction for Node 1020 Case F 5-14

Figure 5-9 Critical Flaw Size Prediction for Node 1020 Case G 5-15

Figure A-1 Pipe With A Through-Wall Crack In Bending A-2

Revision 1 description :

The report is revised for general editorial corrections and to clarify some minor technical comments

1 INTRODUCTION

1.1 BACKGROUND

The current structural design basis for the pressurizer surge line requires postulating non-mechanistic circumferential and longitudinal pipe breaks. This results in additional plant hardware (e.g. pipe whip restraints and jet shields) that would mitigate the dynamic consequences of the pipe breaks. It is, therefore, highly desirable to be realistic in the postulation of pipe breaks for the surge line. Presented in this report are the descriptions of a mechanistic pipe break evaluation method and the analytical results that can be used for establishing that a circumferential type break will not occur within the pressurizer surge line. The evaluations considering circumferentially oriented flaws cover longitudinal cases. The pressurizer surge line is known to be subjected to thermal stratification and the effects of thermal stratification for D. C. Cook Units 1 and 2 surge lines have been evaluated and documented in WCAP-12850 (Reference 1-2) and WCAP-12850 Supplement 1 (Reference 1-3). The results of the stratification evaluation as described in WCAP-12850 and WCAP-12850 Supplement 1 have been used in the Leak-Before-Break evaluation presented in this report.

1.2 SCOPE AND OBJECTIVE

The purpose of this investigation is to demonstrate Leak-Before-Break for the D. C. Cook Units 1 and 2 pressurizer surge lines. The scope of this work covers the entire pressurizer surge line from the primary loop nozzle junction to the pressurizer nozzle junction. A schematic drawing of the piping systems is shown in Section 3.0. The recommendations and criteria proposed in SRP 3.6.3 (Reference 1-4) are used in this evaluation. The criteria and the resulting steps of the evaluation procedure can be briefly summarized as follows:

1. Calculate the applied loads. Identify the location at which the highest stress occurs.

2. Identify the materials and the material properties.

3. Postulate a through-wall flaw at the governing location. The size of the flaw should be large enough so that the leakage is assured of detection with margin using the installed leak detection equipment when the pipe is subjected to normal operating loads. A margin of 10 is demonstrated between the calculated leak rate and the leak detection capability.

4. Using maximum faulted loads, demonstrate that there is a margin of 2 between the leakage size flaw and the critical size flaw.

5. Review the operating history to ascertain that operating experience has indicated no particular susceptibility to failure from the effects of corrosion, water hammer or low and high cycle fatigue.

6. For the materials types used in the plant, provide representative material properties.

7. Demonstrate margin on applied load.

8. Perform an assessment of fatigue crack growth. Show that a through-wall crack will not result.

The leak rate is calculated for the normal operating condition. The leak rate prediction model used in this evaluation is an [

]a,c,e. The crack opening area required for calculating the leak rates is obtained by subjecting the postulated through-wall flaw to normal operating loads (Reference 1-5). Surface roughness is accounted for in determining the leak rate through the postulated flaw.

The computer codes used in this evaluation for leak rate and fracture mechanics calculations have been validated (bench marked).

1.3 REFERENCES

1-1 WCAP-7211, Revision 3, "Energy Systems Business Unit Policy and Procedures for Management, Classification, and Release of Information," June 1994.

1-2 WCAP-12850, "Structural Evaluation of Donald C. Cook Nuclear plant Units 1 and 2 Pressurizer Surge Lines, considering the effects of Thermal Stratification", January 1991.

1-3 WCAP-12850 Supplement 1, "Structural Evaluation of Donald C. Cook Nuclear plant Units 1 and 2 Pressurizer Surge Lines, considering the effects of Thermal Stratification", February 1993.

1-4 Standard Review Plan; public comments solicited; 3.6.3 Leak-Before-Break Evaluation Procedures; Federal Register/Vol. 52, No. 167/Friday, August 28, 1987/Notices, pp. 32626-32633.

1-5 NUREG/CR-3464, 1983, "The Application of Fracture Proof Design Methods Using Tearing Instability Theory to Nuclear Piping Postulating Circumferential Through Wall Cracks."

2 OPERATION AND STABILITY OF THE PRESSURIZER SURGE LINE AND THE REACTOR COOLANT SYSTEM

2.1 STRESS CORROSION CRACKING

The Westinghouse reactor coolant system primary loop and connecting Class 1 Lines have an operating history that demonstrates the inherent operating stability characteristics of the design. This includes a low susceptibility to cracking failure from the effects of corrosion (e.g., intergranular stress corrosion cracking, IGSCC). This operating history totals over 900 reactor-years, including five Plants each having over 20 years of operation and 15 other Plants each with over 15 years of operation.

In 1978, the United States Nuclear Regulatory Commission (USNRC) formed the second Pipe Crack Study Group. (The first Pipe Crack Study Group established in 1975 addressed cracking in boiling water reactors only.) One of the objectives of the second Pipe Crack Study Group (PCSG) was to include a review of the potential for stress corrosion cracking in Pressurized Water Reactors (PWR's). The results of the study performed by the PCSG were presented in NUREG-0531 (Reference 2-1) entitled "Investigation and Evaluation of Stress Corrosion Cracking in Piping of Light Water Reactor Plant." In that report the PCSG stated:

> "The PCSG has determined that the potential for stress-corrosion cracking in PWR primary system piping is extremely low because the ingredients that produce IGSCC are not all present. The use of hydrazine additives and a hydrogen overpressure limit the oxygen in the coolant to very low levels. Other impurities that might cause stress-corrosion cracking, such as halides or caustic, are also rigidly controlled. Only for brief periods during reactor shutdown when the coolant is exposed to the air and during the subsequent startup are conditions even marginally capable of producing stress-corrosion cracking in the primary systems of PWRs.
>
> Operating experience in PWRs supports this determination. To date, no stress-corrosion cracking has been reported in the primary piping or safe ends of any PWR."

During 1979, several instances of cracking in PWR feedwater piping led to the establishment of the third PCSG. The investigations of the PCSG reported in NUREG-0691 (Reference 2-2) further confirmed that no occurrences of IGSCC have been reported for PWR primary coolant systems.

As stated above, for the Westinghouse Plants there is no history of cracking failure in the reactor coolant system loop or connecting Class 1 piping. The discussion below further qualifies the PCSG's findings.

For intergranular stress corrosion cracking (IGSCC) to occur in piping, the following three conditions must exist simultaneously: high tensile stresses, susceptible material, and a corrosive environment. Since some residual stresses and some degree of material susceptibility exist in any stainless steel piping, the potential for stress corrosion is minimized by properly selecting a material immune to IGSCC as well as preventing the occurrence of a corrosive environment. The material specifications consider compatibility with the system's operating environment (both internal and external) as well as other material in the system, applicable ASME Code rules, fracture toughness, welding, fabrication, and processing.

The elements of a water environment known to increase the susceptibility of austenitic stainless steel to stress corrosion are: oxygen, fluorides, chlorides, hydroxides, hydrogen peroxide, and reduced forms of sulfur (e.g., sulfides, sulfates, and thionates). Strict pipe cleaning standards prior to operation and careful control of water chemistry during plant operation are used to prevent the occurrence of a corrosive environment. Prior to being put into service, the piping is cleaned internally and externally. During flushes and preoperational testing, water chemistry is controlled in accordance with written specifications. Requirements on chlorides, fluorides, conductivity, and pH are included in the acceptance criteria for the piping.

During plant operation, the reactor coolant water chemistry is monitored and maintained within very specific limits. Contaminant concentrations are kept below the thresholds known to be conducive to stress corrosion cracking with the major water chemistry control standards being included in the plant operating procedures as a condition for plant operation. For example, during normal power operation, oxygen concentration in the RCS and connecting Class 1 line is expected to be in the ppb range by controlling charging flow chemistry and maintaining hydrogen in the reactor coolant at specified concentrations. Halogen concentrations are also stringently controlled by maintaining concentrations of chlorides and fluorides within the specified limits. This is assured by controlling charging flow chemistry. Thus during plant operation, the likelihood of stress corrosion cracking is minimized.

2.2 WATER HAMMER

Overall, there is a low potential for water hammer in the RCS and connecting surge line since they are designed and operated to preclude the voiding condition in the normally filled surge line. The RCS and connecting surge line including piping and components, are designed for normal, upset, emergency, and faulted condition transients. The design requirements are conservative relative to both the number of transients and their severity. Pressurizer safety and relief valve actuation and the associated hydraulic transients following valve opening are considered in the system design. Only relatively slow transients are applicable to the surge line and there is no significant effect on the system dynamic loads. To ensure dynamic system stability, reactor coolant parameters are stringently controlled. Temperature during normal operation is maintained within

a narrow range; pressure is controlled by pressurizer heaters and pressurizer spray, also within a narrow range for steady-state conditions. The flow characteristics of the system remain constant during a fuel cycle because the only governing parameters, namely system resistance and the reactor coolant pump characteristics, are controlled in the design process. Additionally, Westinghouse has instrumented typical reactor coolant systems to verify the flow and vibration characteristics of the system and connecting surge line. Preoperational testing and operating experience have verified the Westinghouse approach. The operating transients of the RCS primary piping and connected surge line are such that no significant water hammer can occur.

2.3 LOW CYCLE AND HIGH CYCLE FATIGUE

Fatigue considerations are accounted for in the surge line piping through the fatigue usage factor evaluation for the stratification analyses (Reference 1-2) to show compliance with the rules of Section III of the ASME Code. A further assessment of the low cycle fatigue loading is discussed in Section 6.0 as part of this study in the form of a fatigue crack growth evaluation.

Pump vibrations during operation would result in high cycle fatigue loads in the piping system. During operation, an alarm signals the exceeding of the RC pump vibration limits. Field measurements have been made on the reactor coolant loop piping in a number of Plants during hot functional testing. Stresses in the elbow below the RC pump have been found to be very small, between 2 and 3 ksi at the highest. Field measurements on a typical PWR plant indicate vibration amplitudes less than 1 ksi. When translated to the connecting surge line, these stresses would be even lower, well below the fatigue endurance limit for the surge line material and would result in an applied stress intensity factor below the threshold for fatigue crack growth. D. C. Cook configurations are similar and the results are expected to be the same.

2.4 SUMMARY EVALUATION OF SURGE LINE FOR POTENTIAL DEGRADATION DURING SERVICE

There has never been any service cracking or wall thinning identified in the pressurizer surge line of Westinghouse PWR design. Sources of such degradation are mitigated by the design, construction, inspection, and operation of the pressurizer surge piping.

There is no known mechanism for water hammer in the pressurizer/surge system. The pressurizer safety and relief piping system that is connected to the top of the pressurizer could have loading from water hammer events. However, these loads are effectively mitigated by the pressurizer and have a negligible effect on the surge line.

Wall thinning by erosion and erosion-corrosion effects should not occur in the surge line due to the low velocity, typically less than 1.0 ft/sec and the material, austenitic stainless steel, which is highly resistant to these degradation mechanisms. Per

NUREG-0691 (Reference 2-2), a study of pipe cracking in PWR piping, only two incidents of wall thinning in stainless steel pipe were reported and these were not in the surge line. The cause of the wall thinning is related to the high water velocity and is therefore clearly not a mechanism that would affect the surge line.

It is well known that the pressurizer surge line is subjected to thermal stratification and the effects of stratification are particularly significant during certain modes of heatup and cooldown operation. The effects of stratification have been evaluated for the D. C. Cook Units 1 and 2 surge lines and the loads, accounting for the stratification effects, have been derived in WCAP-12850 (Reference 1-2) and WCAP-12850 Supplement 1 (Reference 1-3). These loads are used in the Leak-Before-Break evaluation described in this report.

The D. C. Cook Units 1 and 2 surge line piping systems are fabricated from forged products (see Section 3) which are not susceptible to toughness degradation due to thermal aging.

Finally, the maximum operating temperature of the pressurizer surge piping, which is about 650°F, is well below the temperature that would cause any creep damage in stainless steel piping. Cleavage type failures are not a concern for the operating temperatures and material used in the stainless steel piping of the pressurizer surge lines.

2.5 REFERENCES

2-1 Investigation and Evaluation of Stress-Corrosion Cracking in Piping of Light Water Reactor Plant, NUREG-0531, U.S. Nuclear Regulatory Commission, February 1979.

2-2 Investigation and Evaluation of Cracking Incidents in Piping in Pressurized Water Reactors, NUREG-0691, U.S. Nuclear Regulatory Commission, September 1980.

3 MATERIAL CHARACTERIZATION

3.1 PIPE MATERIAL AND WELDING PROCESS

The pipe material of the pressurizer surge line for the D. C. Cook Units 1 and 2 Nuclear Power Plants is A376/TP316. This is a wrought product of the type used for the primary loop piping of several PWR Plants. The surge line is connected to the primary loop nozzle at one end and the other end of the surge line is connected to the pressurizer nozzle. The surge line does not include any cast pipes or cast fittings. The welding processes used are Gas Tungten Arc Weld (GTAW) and Shielded Metal Arc Weld (SMAW). Figure 3-1 shows the schematic layout of the surge lines and identifies the weld locations by node points.

In the following sections the tensile properties of the materials are presented for use in the Leak-Before-Break analyses.

3.2 MATERIAL PROPERTIES

D. C. Cook Units 1 and 2 Plant specific data was used as a basis for determining tensile properties. The room temperature mechanical properties of the surge line material were obtained from the Certified Materials Test Reports (CMTRs) and are given in Table 3-1. The representative minimum and average tensile properties were established (see Table 3-2). The material properties at temperatures (135°F, 205°F, 617°F and 653°F) are required for the leak rate and stability analyses discussed later. The minimum and average tensile properties were calculated by using the ratio of the ASME Code Section III (Reference 3-1) properties at the temperatures of interest stated above. Table 3-2 shows the tensile properties at various temperatures. The modulus of elasticity values were established at various temperatures from the ASME Code Section III (see Table 3-3). In the Leak-Before-Break evaluation, the representative minimum properties at temperature were used for the flaw stability evaluations and the representative average properties were used for the leak rate predictions. The minimum ultimate stresses were used for stability analyses. These properties are summarized in Table 3-2.

3.3 REFERENCES

3-1 ASME Boiler and Pressure Vessel Code Section III, "Rules for Construction of Nuclear Power Plant Components; Business Unit 2, Appendices", 1989 Edition, July 1, 1989.

Table 3-1 Room Temperature Mechanical Properties of the Pressurizer Surge Line Materials

Heat #	Material	Yield Strength (psi)	Ultimate Strength (psi)
Unit 1			
J-2469 Serial # 6566	A376/TP316	39,800	84,200
J-2469 Serial # 6566	A376/TP316	41,200	86,100
J2471 Serial # 6556	A376/TP316	43.700	88,000
J2471 Serial # 6556	A376/TP316	43,700	88,600
J2470 Serial # 6550	A376/TP316	41,200	84,000
J2470 Serial # 6550	A376/TP316	40,900	84,200
J2469 Serial # 6565	A376/TP316	45,500	87,900
J2469 Serial # 6565	A376/TP316	46,500	87,600
Unit 2			
J2471 Serial # 6557	A376/TP316	38,100	80,200
J2471 Serial # 6557	A376/TP316	39,500	83,400
J2471 Serial # 6551	A376/TP316	41,800	83,400
J2471 Serial # 6551	A376/TP316	39,900	84,300
J2469 Serial # 6563	A376/TP316	45,000	88,100
J2469 Serial # 6563	A376/TP316	44,900	87,100
J2339 Serial # 6311	A376/TP316	41,900	85,900
J2339 Serial # 6311	A376/TP316	42,500	85,900
J2470 Serial # 6549	A376/TP316	41,200	83,100
J2470 Serial # 6549	A376/TP316	41,700	84,300
J2471 Serial # 6556	A376/TP316	43,700	88,000
J2471 Serial # 6556	A376/TP316	43,700	88,600

Table 3-2 Representative Tensile Properties				
Material	**Temperature (°F)**	**Minimum Yield (psi)**	**Average Yield (psi)**	**Minimum Ultimate (psi)**
A376/TP316	Room	38,100	42,320	80,200
	135	36,233	40,246	80,200
	205	32,607	36,219	80,114
	617	23,746	26,377	76,778
	653	23,465	26,063	76,778

Table 3-3 Modulus of Elasticity (E)	
Temperature (°F)	**E (ksi)**
Room	28,300
135	27,950
205	27,570
617	25,215
653	25,035

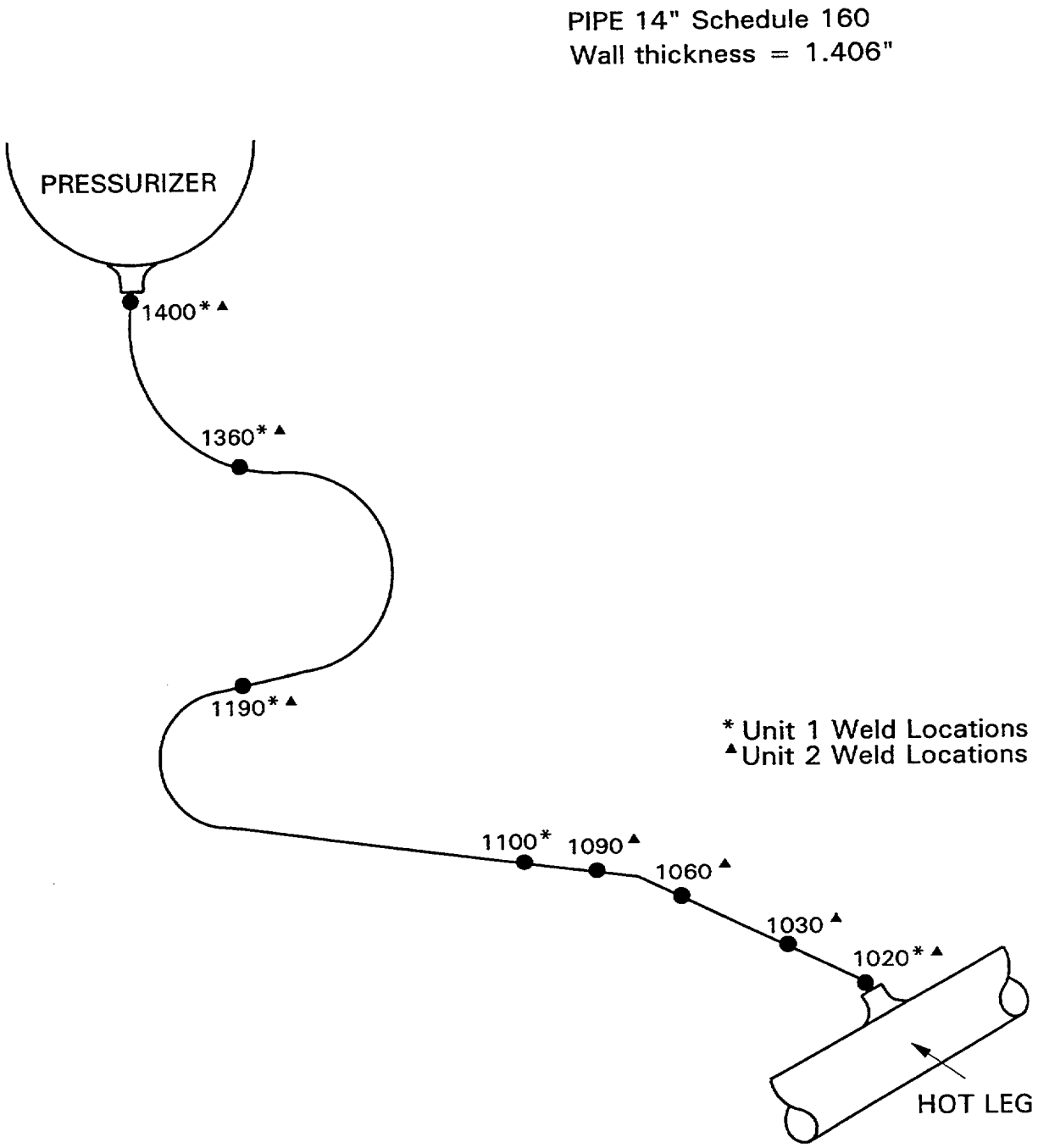

Figure 3-1 D. C. Cook Units 1 and 2 Surge Lines Layout

4 LOADS FOR FRACTURE MECHANICS ANALYSIS

4.1 NATURE OF THE LOADS

Figure 3-1 shows a schematic layout of the surge lines for D. C. Cook Units 1 and 2 and identifies the weld locations.

The stresses due to axial loads and bending moments were calculated by the following equation:

$$\sigma = \frac{F}{A} + \frac{M}{Z} \tag{4-1}$$

where,

σ	=	stress
F	=	axial load
M	=	bending moment
A	=	metal cross-sectional area
Z	=	section modulus

The bending moments for the desired loading combinations were calculated by the following equation:

$$M_B = (M^2_y + M^2_z)^{0.5} \tag{4-2}$$

where,

x axis is along the center line of the pipe.

M_B	=	bending moment for required loading
M_y	=	y component of bending moment
M_z	=	z component of bending moment

The axial load and bending moments for crack stability analysis and leak rate predictions are computed by the methods to be explained in Sections 4.2 and 4.3 which follow.

4.2 LOADS FOR CRACK STABILITY ANALYSIS

The faulted loads for the crack stability analysis were calculated by the absolute sum method as follows:

$$F = |F_{DW}| + |F_{TH}| + |F_p| + |F_{SSE}| \quad (4\text{-}3)$$

$$M_y = |M_{yDW}| + |M_{y\,TH}| + |M_{y\,SSE}| \quad (4\text{-}4)$$

$$M_z = |M_{zDW}| + |M_{z\,TH}| + |M_{z\,SSE}| \quad (4\text{-}5)$$

where

DW = Deadweight

TH = Applicable thermal load (normal or stratified)

P = Load due to internal pressure

SSE = SSE loading including seismic anchor motion

4.3 LOADS FOR LEAK RATE EVALUATION

The normal operating loads for leak rate predictions were calculated by the algebraic sum method as follows:

$$F = F_{DW} + F_{TH} + F_p \quad (4\text{-}6)$$

$$M_y = (M_y)_{DW} + (M_y)_{TH} \quad (4\text{-}7)$$

$$M_z = (M_z)_{DW} + (M_z)_{TH} \quad (4\text{-}8)$$

The parameters and subscripts are the same as those explained in Sections 4.1 and 4.2.

4.4 LOADING CONDITIONS

Because thermal stratification can cause large stresses during heatup and cooldown , a review of stresses was performed to identify the upper bound loadings for Leak-Before-Break applications. The loading states so identified are given in Table 4-1.

Seven loading cases were identified for Leak-Before-Break evaluation as given in Table 4-2. Cases A, B, C are cases for leak rate calculations with the remaining cases being the corresponding faulted situations for stability evaluations.

The cases postulated for Leak-Before-Break are summarized in Table 4-3. The cases of primary interest are the postulation of a detectable leak at normal power conditions

[

]a,c,e

For stratification description, see References 4-1 and 4-2.

The combination [

]a,c,e

The more realistic cases [

]a,c,e

[

] a,c,e is based on the following.

Actual practice, based on experience of other plants with this type of situation, indicates that the plant operators complete the cooldown as quickly as possible once a leak in the primary system is detected. Technical Specifications may require cold shutdown within

36 hours but actual practice is that the plant depressurizes the system as soon as possible once a primary system leak is detected. Therefore, the hot leg is generally on the warmer side of the limits (~200 ^{0}F) when the pressurizer bubble is quenched. Once the bubble is quenched, the pressurizer is cooled down fairly quickly reducing the ΔT in the system.

4.5 SUMMARY OF LOADS

The combined loads were evaluated at the various weld locations. Normal loads were determined using the algebraic sum method whereas faulted loads were combined using the absolute sum method.

4.6 GOVERNING LOCATION

The welds for the D. C. Cook Units 1 and 2 surge Line are fabricated using the GTAW and SMAW procedure. Node 1020 is the governing location, when the stress levels and the weld procedures are both taken into account for all the locations of D. C. Cook Units 1 and 2 pressurizer surge lines. Node 1020 is the highest stressed locations. Figure 4-1 shows the governing location. The loads and stresses at the governing location for all the loading combinations are shown in Table 4-4.

4.7 REFERENCES

4-1 WCAP-12850, "Structural Evaluation of Donald C. Cook Nuclear plant Units 1 and 2 Pressurizer Surge Lines, considering the effects of Thermal Stratification", January 1991.

4-2 WCAP-12850 Supplement 1, "Structural Evaluation of Donald C. Cook Nuclear plant Units 1 and 2 Pressurizer Surge Lines, considering the effects of Thermal Stratification", February 1993.

Table 4-1 Types of Loadings
Pressure (P)
Dead Weight (DW)
Normal Operating Thermal Expansion (TH)
Safe Shutdown Earthquake and Seismic Anchor Motion (SSE)[1]
[ ]a,c,e
[ ]a,c,e
[ ]a,c,e

[1] SSE is used to refer to the absolute sum of these loadings.

Table 4-2 Normal and Faulted Loading Cases for Leak-Before-Break Evaluations	
CASE A	This is the normal operating case at 653°F consisting of the algebraic sum of the loading components due to P, DW and TH.
CASE B	[ ] a,c,e
CASE C	[ ] a,c,e
CASE D	This is the faulted operating case at 653°F consisting of the absolute sum (every component load is taken as positive) of P, DW, TH and SSE.
CASE E	[ ] a,c,e
CASE F	This is a forced cooldown case [ ] a,c,e with stratification [ ] a,c,e
CASE G	[ ] a,c,e

Table 4-3 Associated Load Cases for Analyses	
A/D	This is the heretofore standard leak-before-break evaluation.
A/F	This depicts a postulated forced cooldown resulting from experiencing a detectable leak [ ] a,c,e
B/E	[ ] a,c,e
B/F	This depicts a postulated forced cooldown resulting from experiencing a detectable leak [ ] a,c,e
B/G[1]	[ ] a,c,e
C/G[1]	[ ] a,c,e

1 These are judged to be low probability events.

Table 4-4 Summary of Leak-Before-Break Loads and Stresses by Case for Governing Location

Node	Case	F_X(lbs)	Axial Stress (psi)	M_B(in-lb)	Bending Stress (psi)	Total stress (psi)
1020	A	205,305	3,690	591,740	3,710	7,400
1020	B	207,388	3,728	553,661	3,470	7,198
1020	C	36,746	661	3,110,522	19,500	20,161
1020	D	239,024	4,297	1,743,082	10,930	15,227
1020	E	236,941	4,259	1,916,268	12,010	16,269
1020	F	47,953	862	2,983,880	18,710	19,572
1020	G	51,704	929	4,467,141	28,000	28,929

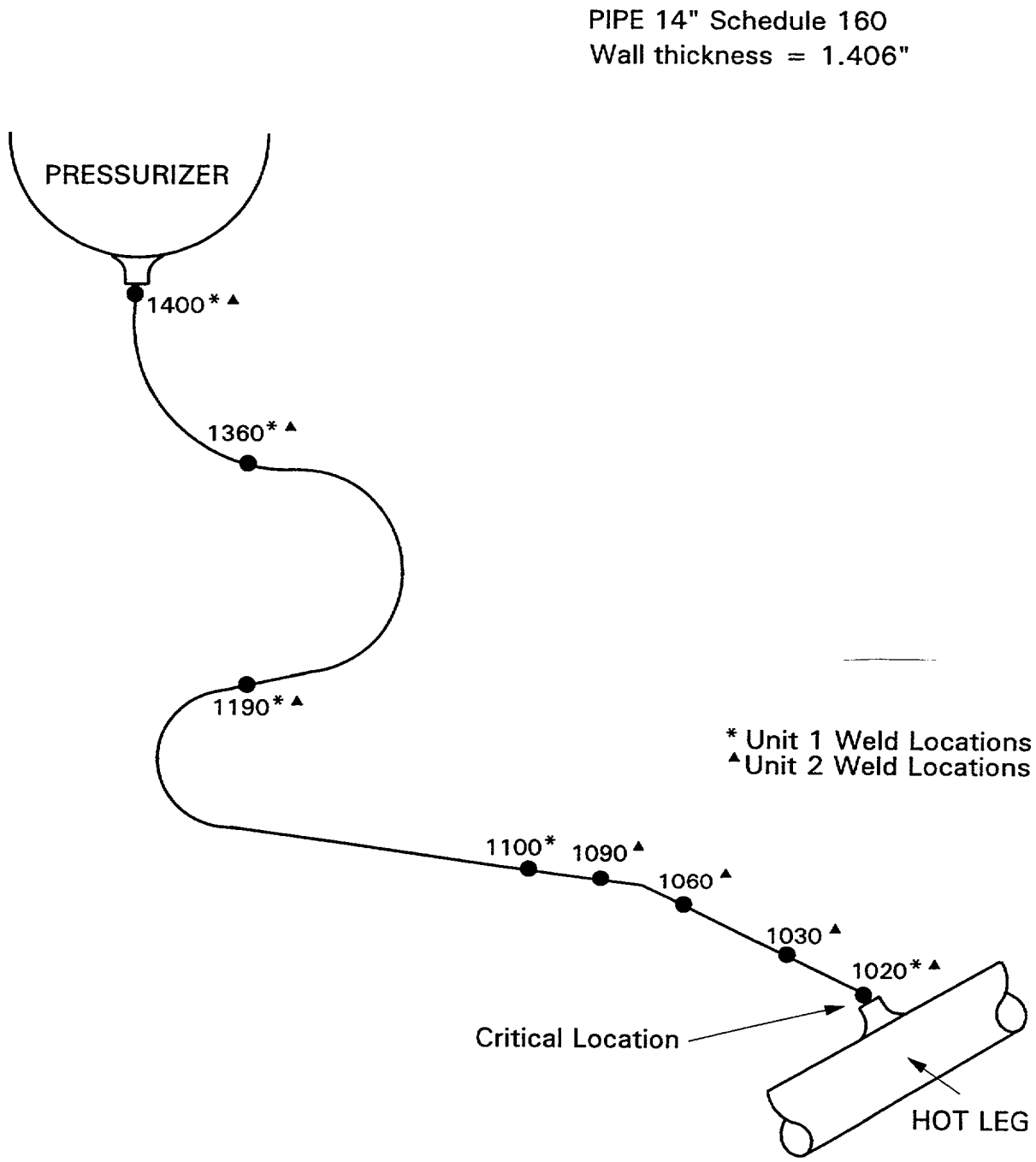

Figure 4-1 D. C. Cook Units 1 and 2 Surge Lines Showing Governing Location

5 FRACTURE MECHANICS EVALUATION

5.1 GLOBAL FAILURE MECHANISM

Determination of the conditions that lead to failure in stainless steel should be done with plastic fracture methodology because of the large amount of deformation accompanying fracture. One method for predicting the failure of ductile material is the [ ]a,c,e method, based on traditional plastic limit load concepts, but accounting for [ ]a,c,e and taking into account the presence of a flaw. The flawed component is predicted to fail when the remaining net section reaches a stress level at which a plastic hinge is formed. The stress level at which this occurs is termed as the flow stress. [

]a,c,e This methodology has been shown to be applicable to ductile piping through a large number of experiments and is used here to predict the critical flaw size in the pressurizer surge line. The failure criterion has been obtained by requiring equilibrium of the section containing the flaw (Figure 5-1) when loads are applied. The detailed development is provided in Appendix A for a through-wall circumferential flaw in a pipe section with internal pressure, axial force, and imposed bending moments. The limit moment for such a pipe is given by:

[ ]a,c,e (5-1)

where:

[

]a,c,e (5-2)

The analytical model described above accurately accounts for the internal pressure as well as an imposed axial force as they affect the limit moment. Good agreement was

found between the analytical predictions and the experimental results (Reference 5-1). Flaw stability evaluations, using this analytical model, are presented in Section 5.3.

5.2 LEAK RATE PREDICTIONS

Fracture mechanics analysis shows that postulated through-wall cracks in the surge line would remain stable and would not cause a gross failure of this component. However, if such a through-wall crack did exist, it would be desirable to detect the leakage such that the plant could be brought to a safe shutdown condition. The purpose of this section is to discuss the method that will be used to predict the flow through such a postulated crack and present the leak rate calculation results for through-wall circumferential cracks.

5.2.1 General Considerations

The flow of hot pressurized water through an opening to a lower backpressure (causing choking) is taken into account. For long channels where the ratio of the channel length, L, to hydraulic diameter, D_H, (L/D_H) is greater than [ ]^{a,c,e}, both [ ]^{a,c,e} must be considered. In this situation the flow can be described as being single-phase through the channel until the local pressure equals the saturation pressure of the fluid. At this point, the flow begins to flash and choking occurs. Pressure losses due to momentum changes will dominate for [ ]^{a,c,e}. However, for large L/D_H values, the friction pressure drop will become important and must be considered along with the momentum losses due to flashing.

5.2.2 Calculational Method

In using the [

]^{a,c,e}.

The flow rate through a crack was calculated in the following manner. Figure 5-2 from Reference 5-2 was used to estimate the critical pressure, Pc, for the primary loop enthalpy condition and an assumed flow. Once Pc was found for a given mass flow, the [ ]^{a,c,e} was found from Figure 5-3 taken from Reference 5-2. For all cases considered, since [ ]^{a,c,e}. Therefore, this method will yield the two-phase pressure drop due to momentum effects as illustrated in Figure 5-4. Now using the assumed flow rate, G, the frictional pressure drop can be calculated using

$$\Delta P_f = [\qquad\qquad]^{a,c,e} \qquad (5\text{-}3)$$

where the friction factor f was determined using the [ ]a,c,e. The crack relative roughness, ε, was obtained from fatigue crack data on stainless steel samples. The relative roughness value used in these calculations was [ ]a,c,e RMS (Reference 5-3).

The frictional pressure drop using Equation 5-3 was then calculated for the assumed flow and added to the [

]a,c,e to obtain the total pressure drop from the system under consideration to the atmosphere. Thus,

$$\text{Absolute Pressure} - 14.7 = [\qquad\qquad]^{a,c,e} \qquad (5\text{-}4)$$

for a given assumed flow G. If the right-hand side of Equation 5-4 does not agree with the pressure difference between the piping under consideration and the atmosphere, then the procedure is repeated until Equation 5-4 is satisfied to within an acceptable tolerance and this results in the flow value through the crack.

For the lower temperature case the leak rate is calculated by using the simple orifice type formula given by Reference 5-4. The pressure drop due to friction is included in predicting the leak rate. The leak rate Q is given by the following equation:

[

] a,c,e

5.2.3 Leak Rate Calculations

Leak rate calculations were performed as a function of postulated through-wall crack length for the critical location previously identified. The crack opening area was estimated using the method of Reference 5-5 and the leak rates were calculated using the calculational methods described above. The leak rates were calculated using the

normal operating loads at the governing location identified in Section 4.0. The crack lengths yielding a leak rate of 10 gpm (10 times the leak detection capability of 1 gpm) for the critical location at the D. C. Cook Units 1 and 2 Nuclear Power Plants' pressurizer surge lines are shown in Table 5-1.

The D. C. Cook Plants RCS pressure boundary leak detection system was determined to meet the criteria previously established for leak detection systems, 1gpm in four hours (Reference 5-6).

5.3 STABILITY EVALUATION

A typical segment of the pipe under maximum loads of axial force F and bending moment M is schematically illustrated in Figure 5-5. In order to calculate the critical flaw size, plots of the limit moment versus crack length are generated as shown in Figures 5-6 to 5-9. The critical flaw size corresponds to the intersection of this curve and the maximum load line. The critical flaw size is calculated using the lower bound base metal tensile properties established in Section 3.0.

The welds at the governing location are GTAW and SMAW. The "Z" factor for GTAW is 1 and therefore, the "Z" factor correction for the SMAW was conservatively applied (Reference 5-7) as follows:

$$Z = 1.15\ [1 + 0.013\ (O.D. - 4)]\ \text{(for SMAW)} \qquad (5\text{-}5)$$

where OD is the outer diameter in inches. Substituting OD = 14.00 inches, the Z factor was calculated to be 1.299 for SMAW. The applied loads were increased by the Z factors and the plots of limit load versus crack length were generated as shown in Figures 5-6 to 5-9. Table 5-2 shows the summary of critical flaw sizes.

5.4 REFERENCES

5-1 Kanninen, M. F. et al., "Mechanical Fracture Predictions for Sensitized Stainless Steel Piping with Circumferential Cracks" EPRI NP-192, September 1976.

5-2 [ ]a,c,e

5-3 "Mechanistic Fracture Evaluation of Reactor Coolant Pipe Containing a postulated circumferential Through-wall Crack," WCAP-9558 Revision 2, May 1981(Westinghouse Class 2).

5-4 [ ] a,c,e

5.4 References (cont'd)

5-5 Tada, H., "The Effects of Shell Corrections on Stress Intensity Factors and the Crack Opening Area of Circumferential and a Longitudinal Through-Crack in a Pipe," Section II-1, NUREG/CR-3464, September 1983.

5-6 Nuclear Regulatory Commission Docket #'s 50-315 and 50-316 Letter from Steven A. Varga, Chief Operating Reactor Branch #1, Division of Licensing, to Mr. John Dolan, Vice President, Indiana and Michigan Electric Company, dated November 22, 1985.

5-7 Standard Review Plan; Public Comment Solicited; 3.6.3 Leak-Before-Break Evaluation Procedures; Federal Register/Vol. 52, No. 167/Friday, August 28, 1987/Notices, pp. 32626-32633.

Table 5-1 Leakage Flaw Size			
Node Point	**Load Case**	**Temperature (°F)**	**Leakage Flaw Size (in.) (for 10 gpm leakage)**
1020	A	653	6.37
1020	B	[ ]a,c,e	6.31
1020	C	[ ]a,c,e	4.22

Table 5-2 Summary of Critical Flaw Size			
Node Point	**Load Case**	**Temperature (°F)**	**Critical Flaw Size (in)**
1020	D	653	16.24
1020	E	[ ]a,c,e	15.79
1020	F	[ ]a,c,e	16.01
1020	G	[ ]a,c,e	12.45

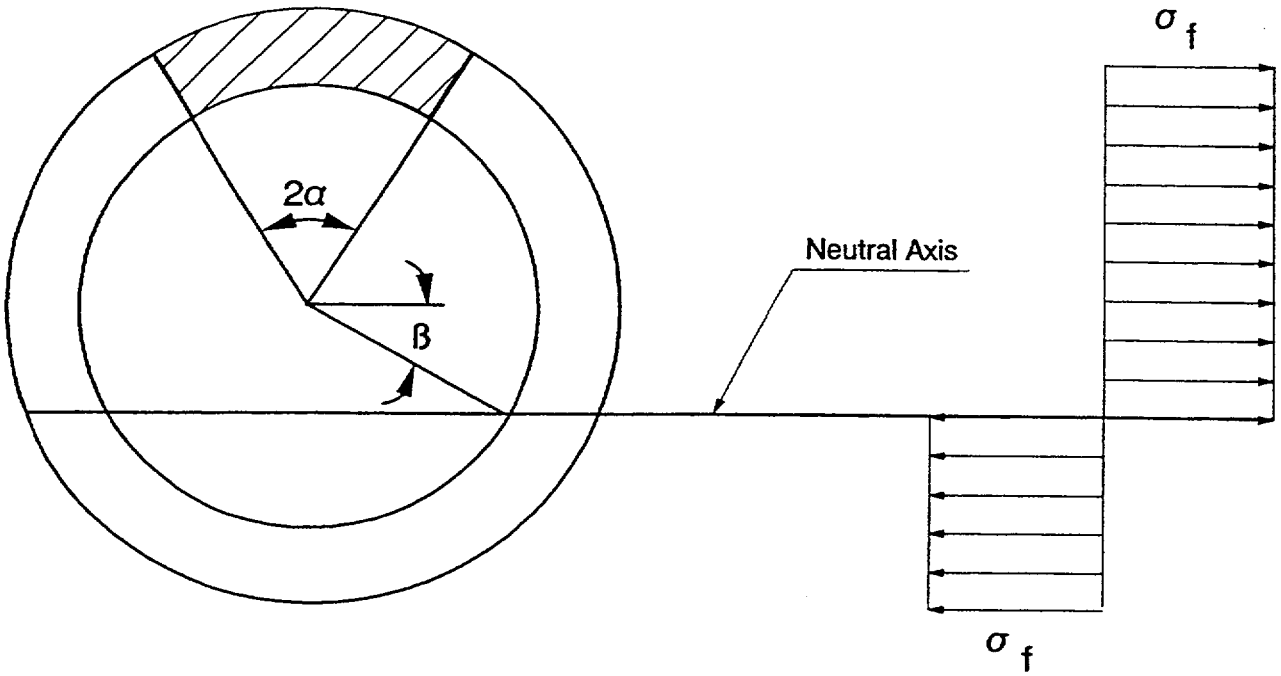

Figure 5-1 Fully Plastic Stress Distribution

a,c,e

[ ]

MASS VELOCITY (lb/(sec)(ft^2))

STAGNATION ENTHALPY (10^2 Btu/lb)

Figure 5-2 Analytical Predictions of Critical Flow Rates of Steam-Water Mixtures

a,c,e

CRITICAL PRESSURE RATIO (p_c/p_o)

LENGTH/DIAMETER RATIO (L/D)

Figure 5-3 [ ]a,c,e Pressure Ratio as a Function of L/D

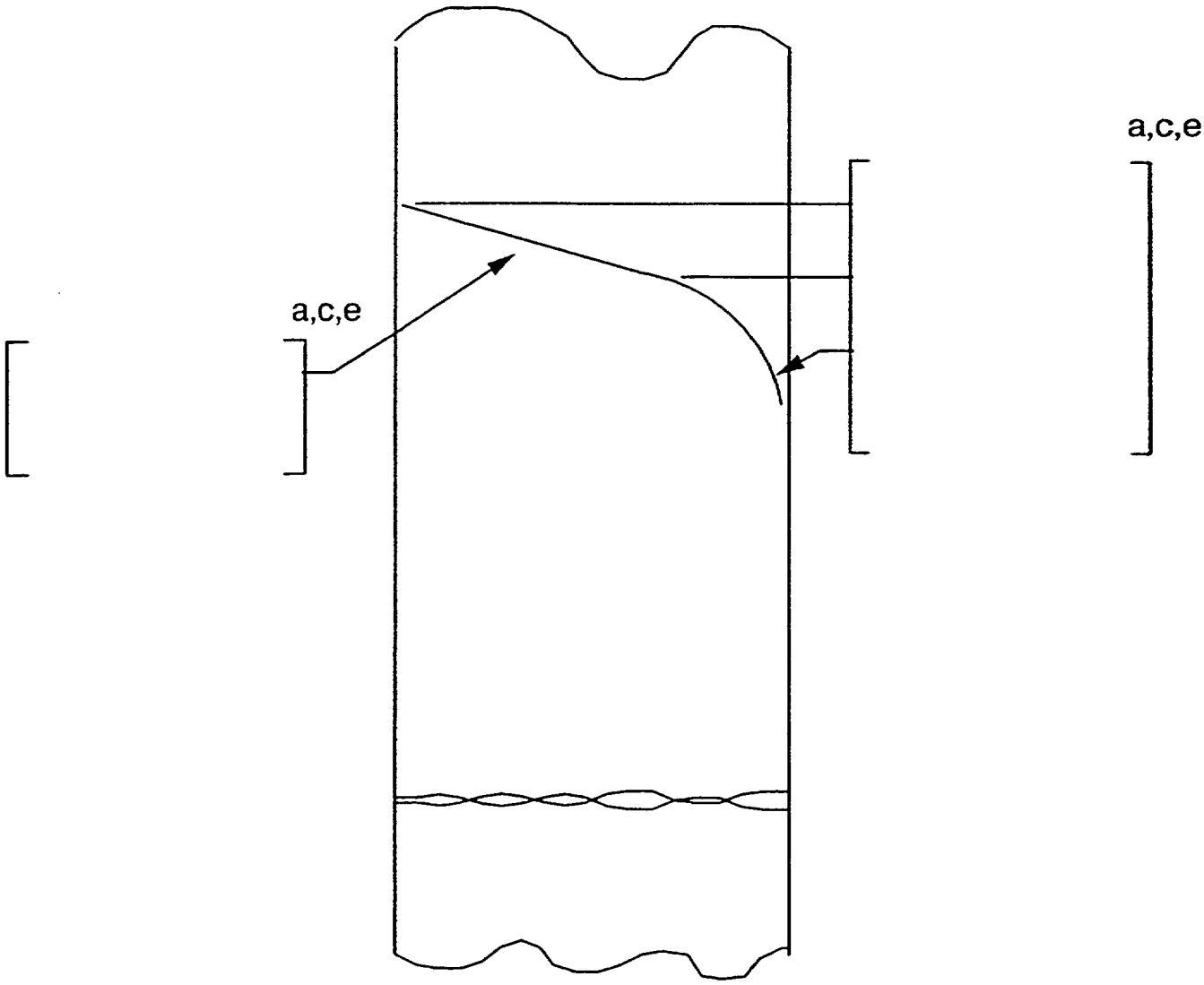

Figure 5-4 Idealized Pressure Drop Profile Through a Postulated Crack

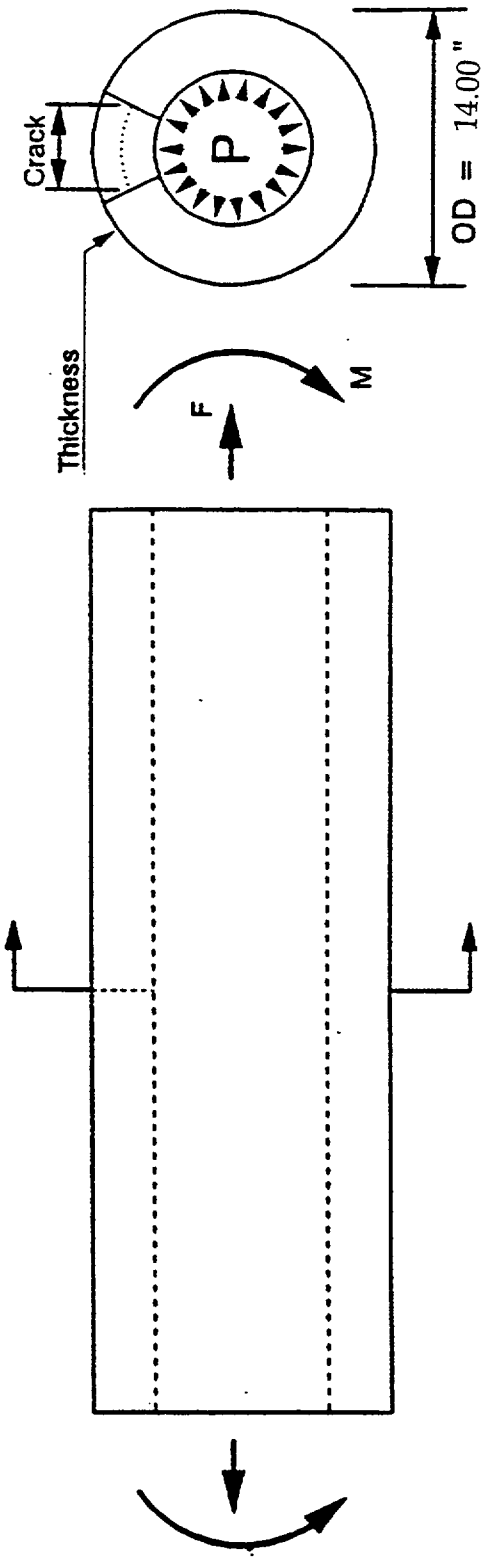

Figure 5-5 Loads Acting on the Model at the Governing Location

a,c,e

[ ]

OD = 14.00 in. σ_y = 23.47 ksi F = 239.02 kips

t = 1.406 in. σ_u = 76.78 ksi M = 1743 in-kips

A376-TP316 with SMAW weld

Figure 5-6 Critical Flaw Size Prediction for Node 1020 Case D

a,c,e

[ ]

OD = 14.00 in. σ_y = 23.75 ksi F = 236.94 kips

t = 1.406 in. σ_u = 76.78 ksi M = 1916 in-kips

A376-TP316 with SMAW weld

Figure 5-7 Critical Flaw Size Prediction for Node 1020 Case E

a,c,e

[ ]

OD = 14.00 in. σ_y = **32.61** ksi F = 47.95 kips

t = 1.406 in. σ_u = **80.11** ksi M = 2984 in-kips

A376-TP316 with SMAW weld

Figure 5-8 Critical Flaw Size Prediction for Node 1020 Case F

a,c,e

OD = 14.00 in. σ_y = 36.23 ksi F = 51.70 kips

t = 1.406 in. σ_u = 80.20 ksi M = 4467 in-kips

A376-TP316 with SMAW weld

Figure 5-9 Critical Flaw Size Prediction for Node 1020 Case G

6 ASSESSMENT OF FATIGUE CRACK GROWTH

6.1 INTRODUCTION

To determine the sensitivity of the pressurizer surge line to the presence of small cracks when subjected to the various transients, a fatigue crack growth analysis was performed for a plant similar to D. C. Cook Units 1 and 2. Fatigue crack growth analysis was performed at two locations. Location 1 was near the reactor coolant loop nozzle and location 2 was also in the vicinity of the reactor coolant loop nozzle.

The results of the fatigue crack growth analysis are presented in Table 6-1. Initial surface flaws were presumed to exist. The flaws were assumed to be semi-elliptical with a six-to-one aspect ratio. The initial flaw assumed was one with a depth equal to 10% of the wall thickness, the maximum flaw size that could be found acceptable by Section XI of the ASME Code. The results show that the maximum fatigue crack growth for 40 years was increased by only ~1%, which is negligible. It was concluded that the fatigue crack growth is not a concern for the pressurizer surge line.

Since the D. C. Cook Units 1 and 2 pressurizer surge line pipe size, pipe schedule and pipe material are the same and the design transients are identical to the plant used in the analysis, it is evident that the D. C. Cook Units 1 and 2 pressurizer surge lines will have similar fatigue crack growth. Although there are some differences in the stratification transients between the typical plant and the D. C. Cook Units 1 and 2 surge lines, those differences will have insignificant impact on the results of the fatigue crack growth and also as indicated above the fatigue crack growth is negligible. Therefore the results shown in Table 6-1 are also representative of the D. C. Cook Units 1 and 2 pressurizer surge line fatigue crack growth.

Table 6-1 Fatigue Crack Growth Results for 10% of Wall Initial flaw Size				
Location	Initial Flaw size (in)	Initial Flaw (% of wall)	Final (40 yr.) Flaw Size (in)	Final Flaw (% of wall)
[				] a,c,e
[				] a,c,e

7 ASSESSMENT OF MARGINS

In the preceding sections, the leak rate calculations, fracture mechanics analysis and fatigue crack growth assessment were performed. Margins at the critical location are summarized below:

In Section 5.3 using the SRP 3.6.3 approach (i.e., "Z" factor approach), the "critical" flaw sizes at the governing location are calculated. In Section 5.2 the crack lengths yielding a leak rate of 10 gpm (10 times the leak detection capability of 1 gpm) for the critical location are calculated. The leakage size flaws, the instability flaws, and margins are given in Table 7-1. The margins are the ratio of instability flaw to leakage flaw. The margins for analysis combination cases A/D, [ ]a,c,e well exceed the factor of 2. The margin for the extremely low probability event defined by [ ]a,c,e also meets the intent of Leak-Before-Break criteria. As stated in Section 4.4, the probability of the simultaneous occurrence of an SSE and maximum stratification loads due to shutdown caused by leakage is estimated to be very low. The faulted loads are combined by absolute summation method and therefore the recommended margin on load is satisfied as per SRP 3.6.3.

In this evaluation, the Leak-Before-Break methodology is applied conservatively. The conservatisms used in the evaluation are summarized in Table 7-2.

Table 7-1 Leakage Flaw Sizes, Critical Flaw Sizes and Margins				
Node	**Load Case**	**Critical Flaw Size (in)**	**Leakage Flaw Size (in)**	**Margin**
1020	A/D	16.24	6.37	2.5
	A/F	16.01	6.37	2.5
	B/E	15.79	6.31	2.5
	B/F	16.01	6.31	2.5
	C/G[1]	12.45	4.22	2.9
	B/G[1]	12.45	6.31	2.0

[1] These are judged to be low probability events

Table 7-2 Leak-Before-Break Conservatisms
Factor of 10 on Leak Rate
Factor of 2 on Leakage Flaw
Algebraic Sum of Loads for Leakage
Absolute Sum of Loads for Stability
Average Material Properties for Leakage
Minimum Material Properties for Stability

8 CONCLUSIONS

This report justifies the elimination of pressurizer surge line pipe breaks as the structural design basis for D. C. Cook Units 1 and 2 Nuclear Power Plants as follows:

a. Stress corrosion cracking is precluded by use of fracture resistant materials in the piping system and controls on reactor coolant chemistry, temperature, pressure, and flow during normal operation.

b. Water hammer should not occur in the RCS piping (primary loop and the attached class 1 auxiliary Line) because of system design, testing, and operational considerations.

c. The effects of low and high cycle fatigue on the integrity of the surge line were evaluated and shown acceptable. The effects of thermal stratification were evaluated and shown acceptable.

d. Ample margin exists between the leak rate of small stable flaws and the capability of D. C. Cook Units 1 and 2 reactor coolant system pressure boundary leakage detection system.

e. Ample margin exists between the small stable leakage flaw sizes of item d and the critical flaw size.

The postulated reference flaw will be stable because of the ample margins in items d and e, and will leak at a detectable rate which will assure a safe plant shutdown.

Based on the above, it is concluded that pressurizer surge line breaks should not be considered in the structural design basis of D. C. Cook Units 1 and 2 Nuclear Power Plants.

APPENDIX A - LIMIT MOMENT

[

]a,c,e

a,c,e

[ ]

Figure A-1 Pipe With A Through-Wall Crack In Bending

ATTACHMENT 4 TO C0800-04

WESTINGHOUSE SUPPLIED INFORMATION
FOR LOADS AT THE THREE HIGHEST STRESS LOCATIONS INCLUDING TORSION,
SAFE SHUTDOWN EARTHQUAKE ACCELERATION LEVEL,
AND PRESSURES AND TEMPERATURES

SAFE SHUTDOWN EARTHQUAKE (SSE) ACCELERATION LEVEL

Leak Before Break (LBB) analysis seismic loads are based on an SSE acceleration level (Containment Elev. 663.3') that corresponds to the Steam Generator upper support elevation.

PRESSURE AND TEMPERATURES USED IN THE LBB ANALYSIS

Table 5-1 and Table 5-2 of WCAP-15434, Revision 1, show the temperatures used for the various load cases. The pressure used for Load Cases A, B, D, and E is 2250 psia and 440 psia is used for Load Cases C, F, and G.

Donald C. Cook Nuclear Plant Units 1 And 2 Pressurizer Surge Lines Additional Loading Information

Loads at the three highest stressed locations are provided below.

NOTE: Node 1030 is the location at which highest ratio of (the loads determined for Case F)-to-(the loads determined for Case B) occurs.

Summary of LBB Loads and Stresses for the Three Highest Stressed Locations

NODE	CASE	AXIAL FORCE (lbs)	BENDING MOMENT (in-lbs)	TOTAL STRESS (psi)
1020	A	205305	591740	7400
1020	B	207388	553661	7200
1020	C	36746	3110522	20160
1020	D	239024	1743082	15220
1020	E	236941	1916268	16270
1020	F	47953	2983880	19570
1020	G	51704	4467141	28930
1030	A	205535	121605	4460
1030	B	207618	221084	5120
1030	C	36976	2660852	17340
1030	D	237876	819157	9410
1030	E	235793	972374	10330
1030	F	47723	2315474	15370
1030	G	50556	3280728	21470
1060	A	205915	310234	5650
1060	B	207998	376637	6100
1060	C	37356	2412553	15800
1060	D	237496	723339	8800
1060	E	235413	707108	8660
1060	F	47343	1989661	13320
1060	G	50176	2623206	17350

Loads With Combined Moment (Including Torsion), M For The Three Highest Stressed Locations

Moment M, is combined as follows:

$M = (M_1^2 + M_2^2 + M_3^2)^{0.5}$

Where M_1 and M_2 are the transverse bending moments and M_3 is the torsional moment.

Summary of LBB Loads for the Three Highest Stressed Locations with Moment, M

NODE	CASE	AXIAL FORCE (lbs)	MOMENT M (in-lbs)
1020	A	205305	614958
1020	B	207388	566105
1020	C	36746	3111380
1020	D	239024	1784816
1020	E	236941	1945222
1020	F	47953	2987835
1020	G	51704	4486479
1030	A	205535	206893
1030	B	207618	250624
1030	C	36976	2661855
1030	D	237876	904560
1030	E	235793	1028248
1030	F	47723	2320569
1030	G	50556	3307009
1060	A	205915	352508
1060	B	207998	394702
1060	C	37356	2413659
1060	D	237496	818797
1060	E	235413	782167
1060	F	47343	1995587
1060	G	50176	2656000

ATTACHMENT 5 TO C0800-04

WESTINGHOUSE APPLICATION LETTER, ACCOMPANYING AFFIDAVIT, PROPRIETARY INFORMATION NOTICE, AND COPYRIGHT NOTICE